

# Northern Gulf of Alaska eddies and associated anomalies

Carol Ladd<sup>a,\*</sup>, Calvin W. Mordy<sup>b</sup>, Nancy B. Kachel<sup>b</sup>, Phyllis J. Stabeno<sup>a</sup>

<sup>a</sup>*Pacific Marine Environmental Laboratory, NOAA, 7600 Sand Point Way, Seattle, WA 98115 6349, USA*

<sup>b</sup>*Joint Institute for the Study of the Atmosphere and Ocean, University of Washington, USA*

Received 9 February 2006; received in revised form 18 January 2007; accepted 26 January 2007

Available online 14 February 2007

## Abstract

In recent years, large anticyclonic eddies have been observed quasi-annually in the region seaward of Kodiak Island, Alaska. In situ sampling in 3 of these eddies was undertaken in 2002, 2003, and 2004. Satellite altimetry data showed that these 3 eddies had 3 different formation regions but their translation pathways were similar near Kodiak Island. Eddies in this region can persist for several years, moving southwestward along the Alaskan Peninsula to the Aleutian Archipelago. Water properties in the cores of the 2003 and 2004 eddies were significantly different from each other, probably because the 2003 eddy formed on the shelf near Yakutat while the 2004 eddy formed farther out in the basin in the northern Gulf of Alaska. Calculation of heat, salinity, and nutrient anomalies associated with the eddies showed that, in their subsurface core waters, the eddies carry excess heat, salt, nitrate and silicic acid seaward from the eddy formation regions.

© 2007 Elsevier Ltd. All rights reserved.

*Keywords:* Oceanic eddies; USA; Alaska; Gulf of Alaska; Satellite altimetry; Shelf-slope exchange

## 1. Introduction

Mesoscale eddies have been hypothesized to be an important mechanism for cross-shelf exchange in the northern Gulf of Alaska (GOA) near Kodiak Island (Okkonen et al., 2003; Ladd et al., 2005a). Examination of altimetry data shows that these eddies generally form in late fall or winter in the eastern GOA and translate around the head of the gulf, staying within ~200 km of the shelf-break. They influence cross-shelf exchange in 2 ways: (1) by trapping coastal waters in their interior during formation with subsequent transport into the basin and (2) through interaction with the shelf-break

current due to their proximity to the shelf-break during their life cycle. As an example of the 1st cross-shelf exchange mechanism, Ladd et al. (2005b) showed that the core waters of an eddy sampled in 2003 near Kodiak Island had water properties consistent with the shelf region near Yakutat (see Fig. 1 for map), suggesting that these waters had been transported hundreds of kilometers from the eddy's formation region. As an example of the 2nd mechanism, Okkonen et al. (2003) compared satellite altimetry and hydrographic data to examine the influence of an eddy on cross-shelf transport in the spring of 1999. They found that cross-slope gradients were strengthened at the leading and trailing edges and weakened (promoting shelf-slope exchange) where the eddy was adjacent to the shelf.

Eddies in the GOA appear to be important to the ecosystems of the region. Their influence on

\*Corresponding author. Tel.: +1 206 526 6024;  
fax: +1 206 526 6485.

E-mail address: [carol.ladd@noaa.gov](mailto:carol.ladd@noaa.gov) (C. Ladd).

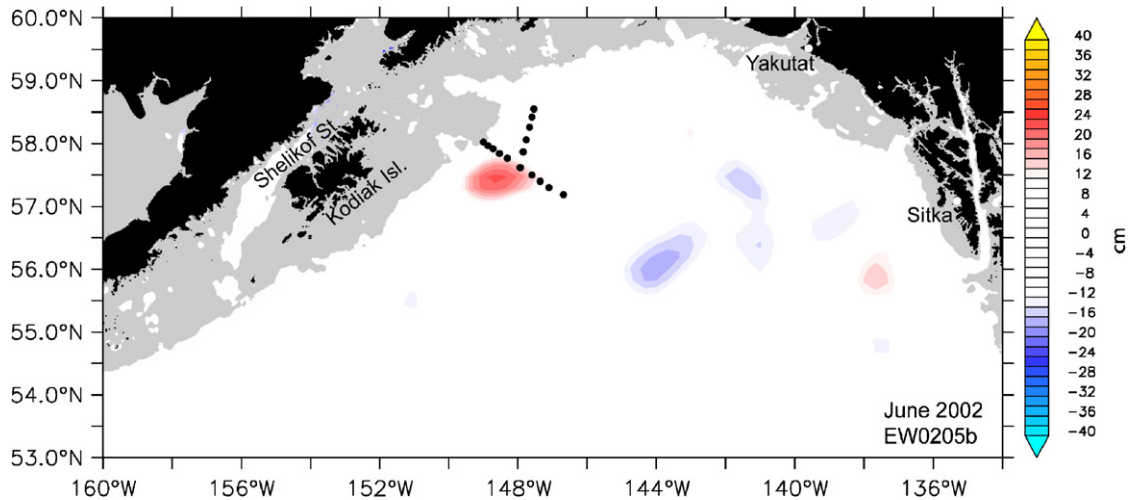


Fig. 1. Location of CTD transects across the 2001 eddy (black dots) plotted over SSHA on the date of the transect (color). SSHA in water shallower than 200 m is not shown.

cross-shelf exchange may have important implications for the distribution of micro- and macro-nutrients and biota. They have been shown to influence the distribution of phytoplankton biomass (Brickley and Thomas, 2004) and the foraging patterns of fur seals (Ream et al., 2005). The Haida eddy, in the southeastern GOA has been shown to influence chlorophyll (Crawford et al., 2005) and zooplankton (Mackas and Galbraith, 2002) distributions. The Sitka eddy may influence sockeye salmon migration patterns (Healey et al., 2000).

Okkonen et al. (2001) used altimetry data from GEOSAT (fall 1986–1989), ERS-1 (spring 1992–winter 1993) and TOPEX (fall 1992–summer 1995) along with model simulations to examine the formation and evolution of eddies in the GOA. They noted 2 preferred formation regions (near Sitka and Yakutat, Alaska) for eddies in the northern GOA. Okkonen et al. (2001) also discuss Haida eddies, formed farther south, near the Queen Charlotte Islands, British Columbia. These eddies usually translate westward into the basin and do not influence the GOA north of  $\sim 55^\circ\text{N}$ . Thus, Haida eddies will not be discussed further.

The Sitka and Yakutat eddies often translate around the northern GOA, eventually interacting with the Alaskan Stream, the western boundary current of the eastern North Pacific subpolar gyre. The Alaskan Stream flows southwestward along the shelf-break from the head of the GOA to the central Aleutian Islands. Crawford et al. (2000) used 6 years

of TOPEX/Poseidon altimetry data to examine the lifecycles of eddies in the Alaskan Stream. They showed that these eddies have sea surface height anomalies up to 72 cm and diameters of  $\sim 160$  km, and can live up to 3 years. Of the 6 eddies they tracked, only 2 had their entire life within the time window of the altimetry dataset available at the time (1992–1998). One of these was formed near Sitka, Alaska in April 1996 and the other was formed in January 1995 in the northeastern GOA near  $59^\circ\text{N}$ .

In recent years (2000–2004), a large eddy has been present in the region seaward of Kodiak Island every spring. From 1992 to 1999, eddies in the region were less frequent (averaging 1 eddy with maximum SSHA  $> 20$  cm every 2 years). In situ sampling in these eddies was undertaken in this region in 2002–2004. The eddy sampled in 2002 formed in 2001 (hereafter called the 2001 eddy) while the other 2 eddies were 1st sampled in their initial year. Ladd et al. (2005b) presented data from the formation year of the 2003 eddy suggesting that it formed near Yakutat. This eddy was sampled again in 2004 allowing a more thorough description of its interannual evolution. Through a combination of in situ and satellite data, we update the description of the 2003 Yakutat eddy (Ladd et al., 2005b) and characterize the lifecycle, translation, water properties, etc. of all 3 eddies. In addition, we calculate the heat, salinity and nutrient anomalies associated with the eddies to quantify the influence of eddies on the surrounding basin waters.

## 2. Methods

### 2.1. In situ data

Three northern Gulf of Alaska eddies were sampled during 6 separate research cruises over the course of 3 years (Table 1). On most cruises (exception noted below), conductivity/temperature/depth (CTD) data were obtained with a SeaBird 911 plus CTD equipped with dual temperature and conductivity sensors. Salinity samples were taken on each cast to calibrate the CTD. During the EW0409 cruise in October 2004, the pump on the CTD failed, making salinity measurements questionable. In response, a pumped SBE 19 CTD was attached to the rosette frame to provide another source of salinity data. In general, the 2 instruments were in good agreement below 100 m but data from the unpumped 911 plus were noisy in the upper 100 m. Thus, data from the SBE 19 were used in the upper 100 m. The quality of these data is not as good as a pumped SeaBird 911 plus and some outliers had to be removed. Thus, the salinity data from this cruise are of lower quality than the rest of the data reported on in this manuscript. In any case, data at densities less than  $25.5 \text{ kg m}^{-3}$  (depths shallower than approximately 80 m in the eddy core water) were not used in the anomaly calculations of Section 6.

On each cast, Niskin bottles were sampled for nutrients (nitrate, nitrite, phosphate and silicic

acid). Nutrient analysis was conducted on board the ship only during the KM0309 and KM0313 cruises. On other cruises, samples were frozen, and returned to the laboratory for analysis. However, data collected from frozen samples were too noisy to be useful in this analysis. Nutrients were analyzed using protocols from the World Ocean Circulation Experiment (WOCE)/Joint Global Ocean Flux Study (JGOFS) (Gordon et al., 1994).

Near-real-time altimetry data from the Colorado Center for Astrodynamic Research (<http://e450.colorado.edu/realtime/welcome/>) and/or from Aviso (<http://www.aviso.oceanobs.com/>) were used to give an initial estimate of the location of the eddy center. However, depending on the translation speed of the eddy, center locations estimated from altimetry data can give errors of  $> 50 \text{ km}$ , and thus are not precise enough to ensure sampling of the eddy core water (Ladd et al., 2005b). To increase the likelihood of sampling close to the center of the eddies, satellite-tracked ARGOS drifters were usually deployed in the eddies prior to conducting the transect. For those transects where drifter data were available prior to sampling, the drifter data enabled us to direct the ships to sample very close ( $< 20 \text{ km}$ ; sometimes within  $5 \text{ km}$ ) to the eddy center. Even when drifter data were not available prior to conducting the CTD transect, data from drifters deployed during the transect allowed an a posteriori estimate of transect position relative to the eddy location.

Table 1  
Eddy cruises

Cruise (ship)	Date	Eddy sampled	Distance from center (km)	Drifters deployed
EW0205b (R.V. <i>Maurice Ewing</i> )	1–3 Jun 2002	2001	$> 50$	36 261 36 263
KM0309 (R.V. <i>Kilo Moana</i> )	14–16 May 2003	2003	$< 8$	37 492 37 504
KM0313 (R.V. <i>Kilo Moana</i> )	25–27 Sep 2003	2003	$< 2$	37 499 37 516
HX284 (cross-shelf) (R/V <i>Alpha Helix</i> )	19–21 May 2004	2003	$< 15$	43 726
HX284 (along-shelf) (R.V. <i>Alpha Helix</i> )	21–22 May 2004	2003	$< 6$	43 725
EW0409 (R.V. <i>Maurice Ewing</i> )	3–5 Oct 2004	2003	No drifter data	None
HX284 (R.V. <i>Alpha Helix</i> )	23–24 May 2004	2004	$> 50$	43 720
HX287 (R.V. <i>Alpha Helix</i> )	10–12 Jul 2004	2004	$< 8$	43 698 43 719
EW0409 (R.V. <i>Maurice Ewing</i> )	29 Sep–2 Oct 2004	2004	No drifter data	None

The 2001 eddy was sampled in early June 2002 (Fig. 1). Unfortunately, the transect missed the eddy center by more than 50 km as drifter data were not available prior to the transect. The 2003 eddy was sampled on 4 cruises: spring and autumn of 2003 and spring and autumn of 2004 (Fig. 2), providing an unprecedented examination of the interannual evolution of a northern GOA eddy. Some of the data from 2003 were previously discussed by Ladd et al. (2005b). The 2004 eddy was sampled with 3 CTD transects in May, July, and October 2004 (Fig. 3). The May 2004 transect missed the center of the eddy by more than 50 km (Table 1).

## 2.2. Altimetry data

Gridded sea level anomalies were downloaded from Aviso. The “ref merged” dataset (obtained from <http://www.jason.oceanobs.com>) consists of merged data from 2 satellite missions, Topex/Poseidon and ERS, followed by Jason-1 and Envisat. This dataset has stable sampling in time (SSALTO/DUACS, 2006). The optimal interpolation methodology used by Aviso to merge data from multiple altimeters is described by Le Traon et al. (1998). The dataset available at the time this paper was completed included data from October 1992 to January 2006. Before August 2002, this product includes data from the Topex/Poseidon and ERS-1 or ERS-2 satellites. From August 2002 to June 2003, Jason-1 and ERS-2 were used. After June 2003, the Jason-1 and ENVISAT satellites were used (SSALTO/DUACS, 2006). The mapped altimetry data set includes 1 map every 7 days with a  $1/3^\circ$  spatial resolution on a Mercator grid (Ducet et al., 2000; Le Traon and Dibarboure, 1999). Merging data from multiple satellites with differing spatial and temporal resolution helps resolve the mesoscale allowing for a better description of eddy activity (Ducet et al., 2000; Le Traon and Dibarboure, 2004).

Sea surface height anomalies (SSHA) from satellite altimeters include a large-scale seasonal cycle made up primarily of expansion/contraction of the water column due to seasonally varying heat flux forcing. A monthly climatology of SSHA (calculated as a simple average of all January data, all February data, etc) (Fig. 4) exhibits higher SSHA in the center of the GOA in summer and lower in winter. However, because the distribution of eddies in this region is seasonally dependent, an eddy signal also is observed in the climatology. Smooth-

ing the climatology over a spatial scale of  $\sim 200$  km reduces the influence of eddies. SSHA discussed in the remainder of this paper have had the smoothed monthly climatology removed.

## 2.3. Satellite-tracked drifters

Satellite-tracked ARGOS drifters, drogued at 40 m with “holey sock” drogues, were deployed. Some of these drifters were specifically deployed in an eddy in an attempt to track flow within the eddy. Other drifters were deployed upstream and were entrained into 1 of the eddies. Drifter data were used to increase the precision of eddy center location estimates in order to direct the in situ sampling, to estimate the location of the in situ sampling relative to the eddy center, and to provide information regarding flow patterns, speeds, and residence times in and around the eddies. ARGOS position fixes can have errors of 100–300 m which would result in velocity errors less than  $5 \text{ cm s}^{-1}$  (Bograd et al., 1999). Wind slippage results in errors of less than  $1 \text{ cm s}^{-1}$  in  $10 \text{ m s}^{-1}$  winds (Niiler et al., 1995).

Position data received from the ARGOS system were examined and obviously erroneous positions were deleted. Position fixes within 15 min of each other were averaged. Since positions were measured at irregular intervals, a linear interpolation was applied to the data, which were then resampled at hourly intervals. Centered differences were used to calculate drifter velocities.

## 3. 2001 eddy

Time constraints restricted the sampling in June 2002 to 1 transect across the eddy. During the transect, 2 drifters were deployed in the eddy. The 1st circuit transcribed by these drifters (1–9 June 2002) allowed an estimate of the location of the center of the eddy ( $57.4^\circ\text{N}$ ,  $149.0^\circ\text{W}$ ). Unfortunately, because of the lack of drifter data prior to the transect, the hydrographic transect missed the center by  $\sim 50$  km and therefore did not sample the core water of the eddy. (Ladd et al. (2005b) showed that the core waters of the 2003 eddy can only be observed within  $\sim 40$  km from the center.) However, after the June 2002 cruise, multiple drifters transited around the 2001 eddy over its lifetime. Data from these drifters and from satellite altimetry were used to examine this eddy and compare it to the 2003 and 2004 eddies, which were more thoroughly observed in situ.

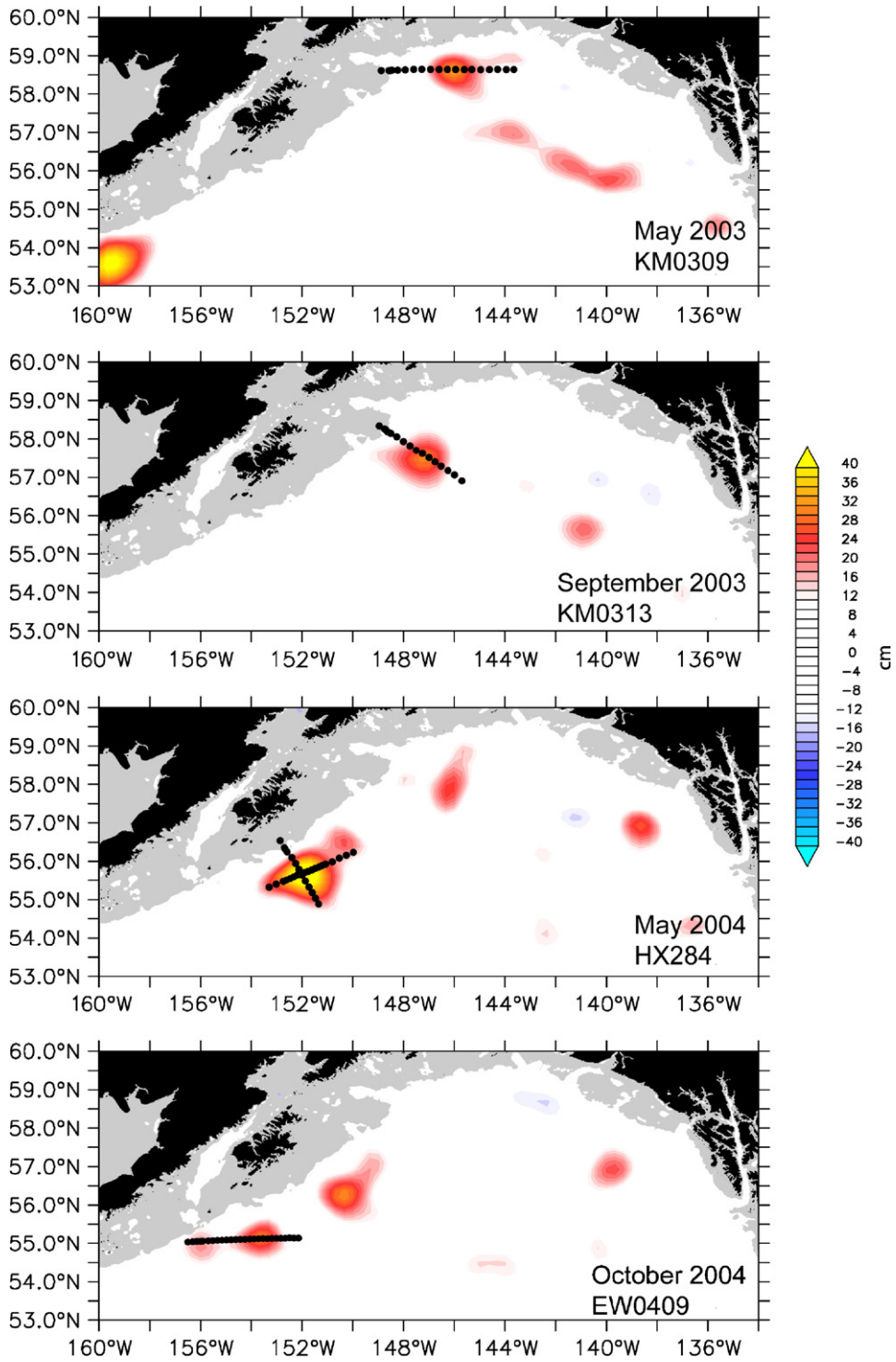


Fig. 2. Location of CTD transects across the 2003 eddy (black dots) plotted over SSHA on the date of the transect (color). SSHA in water shallower than 200 m is not shown.

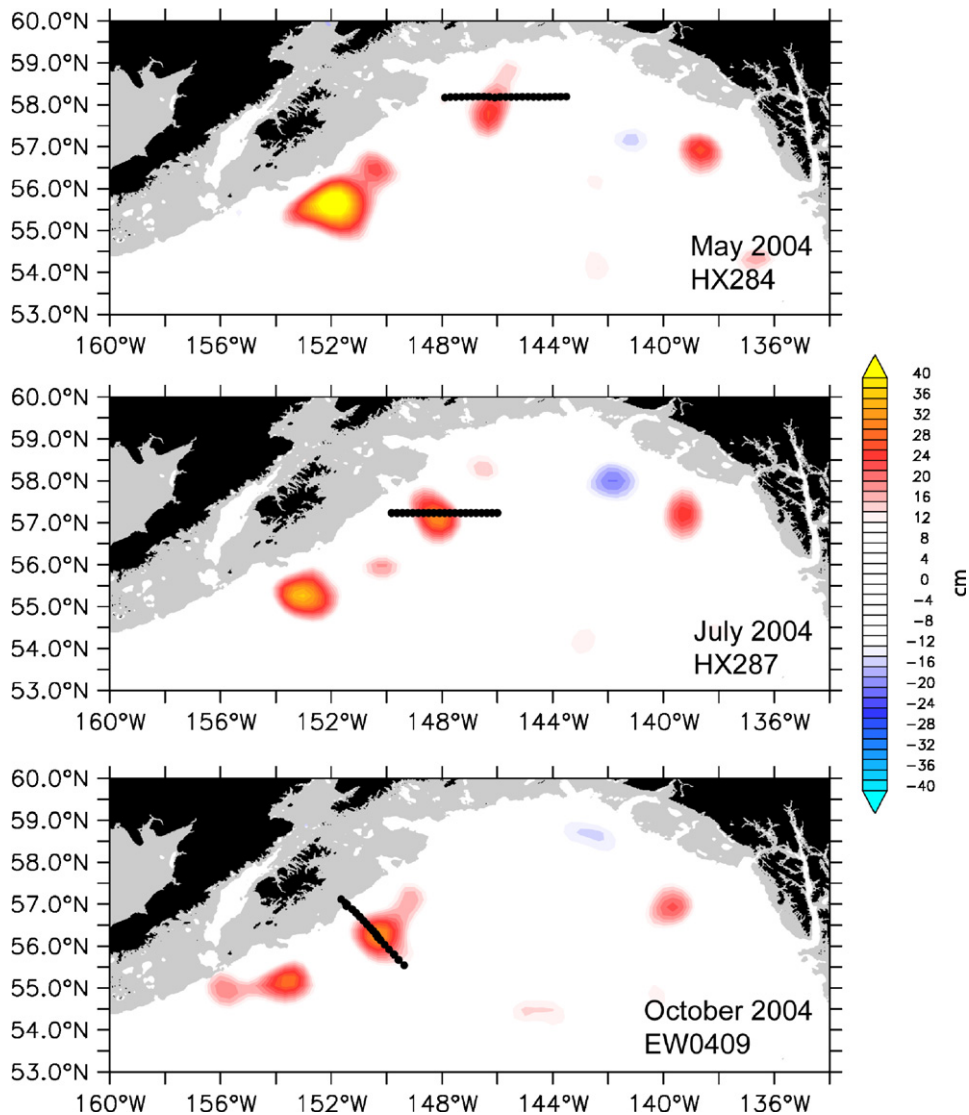


Fig. 3. Location of CTD transects across the 2004 eddy (black dots) plotted over SSHA on the date of the transect (color). SSHA in water shallower than 200 m is not shown.

Using altimetry data, the 2001 eddy can be tracked to determine its formation time and location and its trajectory (Fig. 5). The eddy was 1st observed in the altimetry data in January 2001 centered at approximately 56.9°N, 137°W (the formation location of Sitka eddies; Tabata, 1982). In its 1st year, it moved northwestward, staying approximately 100 km offshore of the 200 m isobath (shelf-break). In the winter of 2001/2002, the diameter of the 15 cm SSHA contours (Fig. 5) decreased, suggesting that the eddy had weakened. This weakening could have been due to energy exchanges with the Alaskan Stream in which it is

embedded or due to the decay of the eddy by diffusion.

Monthly translation speeds during the 1st year (2001) averaged 2.0 km day<sup>-1</sup> (2.3 cm s<sup>-1</sup>) (Table 2). Translation speed averaged over 2002 increased to 2.9 km day<sup>-1</sup> (3.4 cm s<sup>-1</sup>), possibly because of interaction with the Alaskan Stream, which has speeds on the order of 50–100 cm s<sup>-1</sup> (Reed and Stabeno, 1989). In January 2003, after passing the exit of Shelikof Strait, the eddy strengthened with maximum SSHA averaging 46 cm during 2003, and increasing still more to 50 cm in 2004. In early February 2005, the 2001 eddy split into 2 eddies.

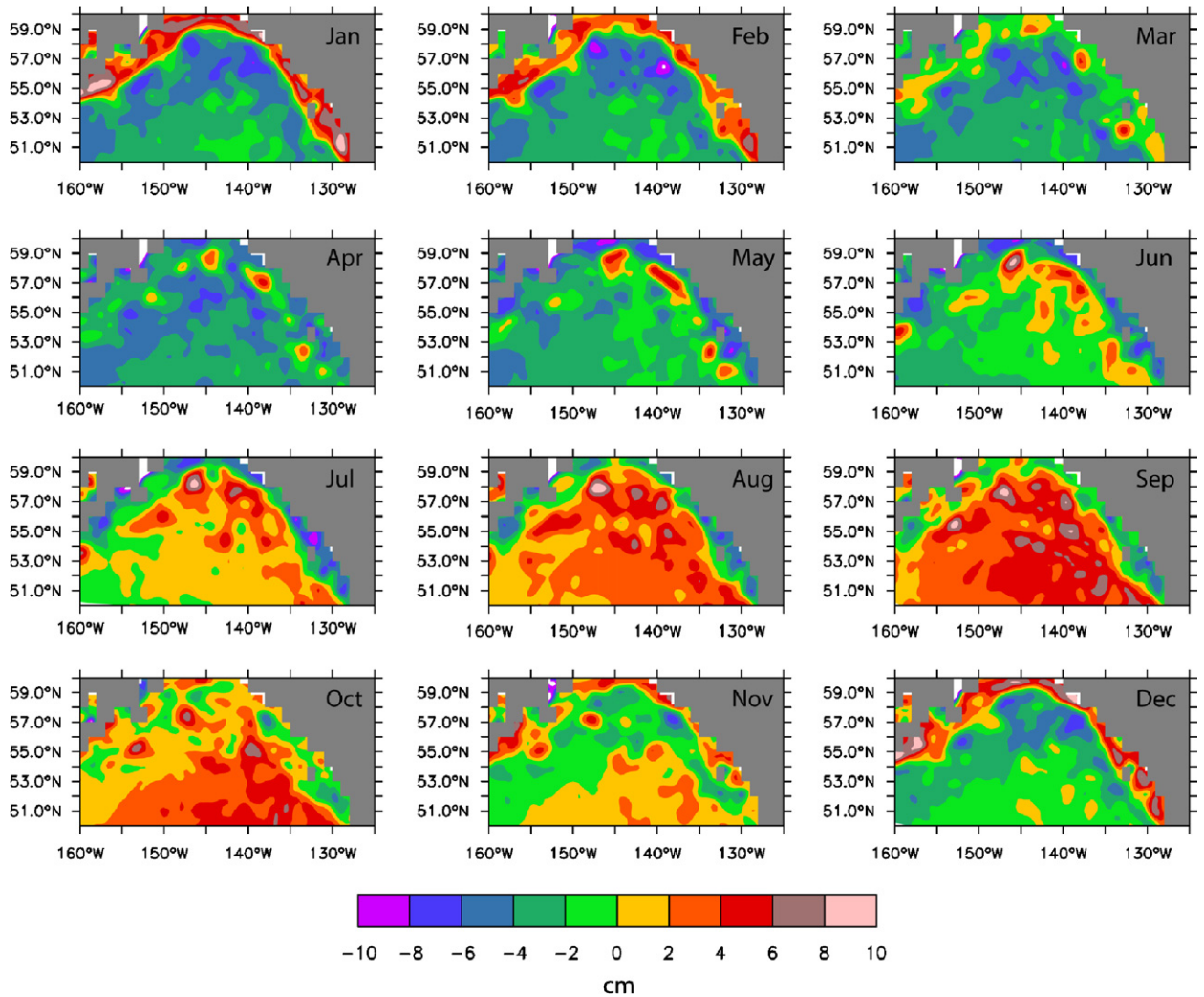


Fig. 4. Monthly climatology of SSHA calculated as a simple average of all January data, all February data, etc.

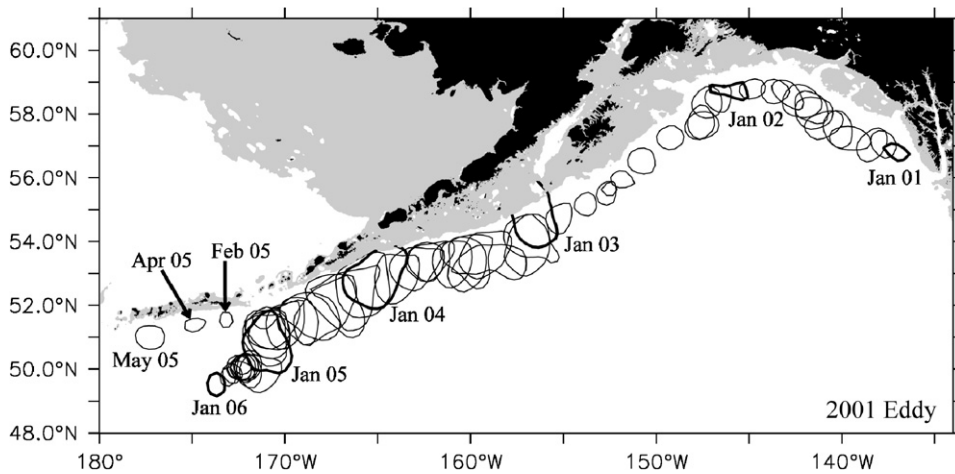


Fig. 5. SSHA 15cm contours (except for January 2001 and January 2006: 10 cm contours) associated with the 2001 eddy plotted on the 15th of each month. January contours are bold.

The smaller sub-eddy continued to move westward along the Aleutians, finally disappearing in early June 2005. The larger sub-eddy moved southward away from the Aleutians and the Alaskan Stream. As of January 2006, this sub-eddy was still in existence with a maximum SSHA  $\sim 15$  cm near  $50^\circ\text{N}$ ,  $172^\circ\text{W}$ . The lifetime of the 2001 eddy has been at least 61 months making it the longest-lived northern GOA eddy in the altimetry record (since 1992).

SeaWiFS data from May 2002 showed a ribbon of high chlorophyll, apparently originating on the shelf, wrapped around the outside of the 2001 eddy

Table 2  
Translation and maximum SSHA from altimetry

	2001 Eddy	2003 Eddy	2004 Eddy <sup>a</sup>
<i>Average translation speed (km/day)</i>			
2001	2.0		
2002	2.9		
2003	2.4	1.7	
2004	2.2	1.7	3.3
2005	1.1	2.5	1.7
<i>Maximum SSHA averaged over year (cm)</i>			
2001	27		
2002	27		
2003	46	33	
2004	50	37	30
2005	26	36	20

<sup>a</sup>Speed and SSHA for 2004 eddy was averaged over May 2004–March 2005 (the lifetime of this eddy).

(Fig. 6). East of the eddy, another long filament of high chlorophyll extended from the shelf into the gulf, wrapping around another sea surface height maximum. However, not all high chlorophyll in the basin appears to be related to eddies. Using 4 years of SeaWiFS data, Brickley and Thomas (2004) showed that eddies in this region contribute to increased chlorophyll concentrations each spring extending up to 300 km offshore of the shelf-break. The increased concentrations of phytoplankton associated with these eddies likely influences the entire ecosystem. A female fur seal was observed to pause in her winter 2002/2003 migration from the Bering Sea to the coastal region of Washington/British Columbia in order to forage in the 2001 eddy (Ream et al., 2005; see their Fig. 9), suggesting that the eddy provided a rich foraging area.

Twelve drifters circled around the 2001 eddy at various times during 2002 and 2003. Most of the drifters were pulled seaward of the shelf-break by the eddy, looped around the outside edge of the eddy, and continued along with the Alaskan Stream. One drifter (37 512) made at least 4 circuits around the eddy over the course of 2 months in 2003 (Fig. 7). The 1st 3 circuits had periods of 8 days at radii averaging  $\sim 44$  km. The speeds experienced by the drifter (calculated from hourly position data) were as high as  $70 \text{ cm s}^{-1}$  (averaging  $\sim 40 \text{ cm s}^{-1}$ ) and were faster on the southern side of the eddy. During the last full circuit before exiting the eddy, the drifter was at a radius of  $\sim 75$  km. During this 2 month period, the eddy was almost stationary

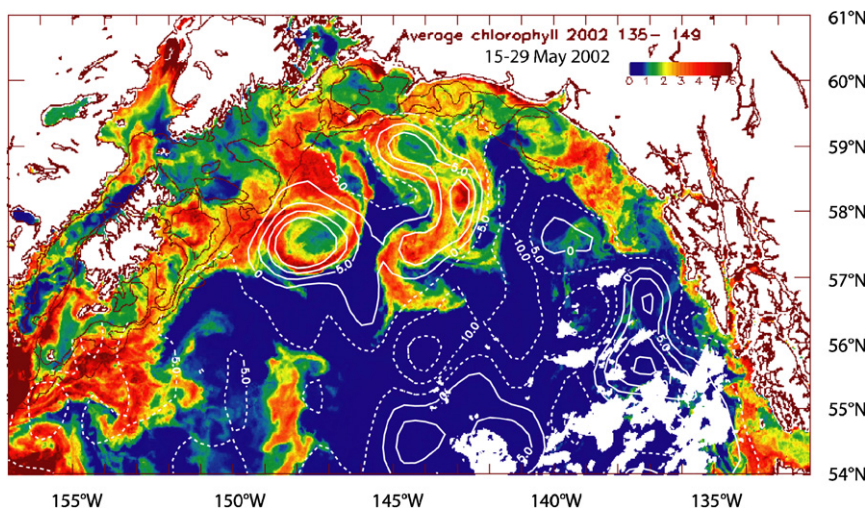


Fig. 6. Surface chlorophyll-*a* ( $\text{mg m}^{-3}$ ) averaged over 15–29 May 2002 from the SeaWiFS satellite. SSHA contours (white) for the same period are overlaid. Contour interval = 5 cm. Negative SSHA are dashed.



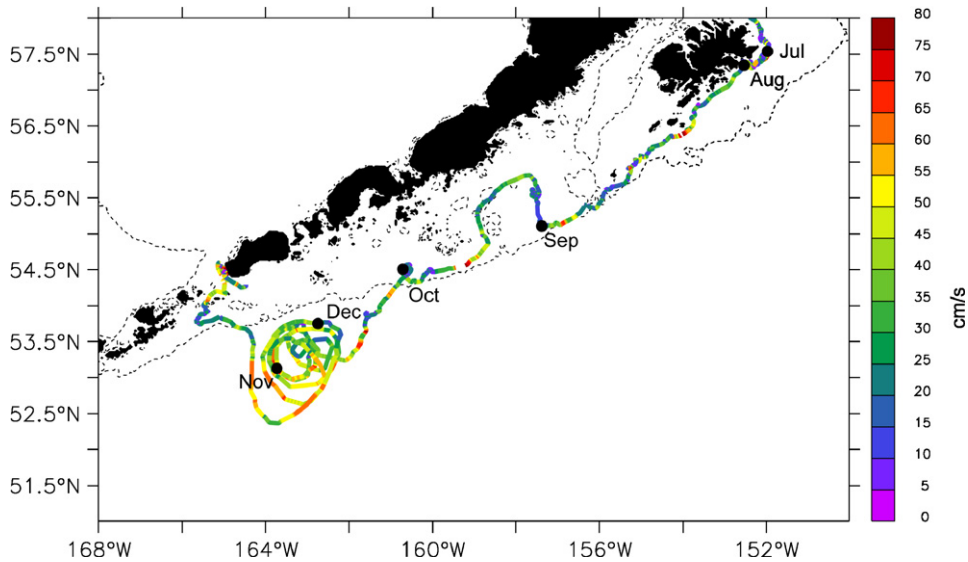


Fig. 7. Trajectory of drifter 37512 in 2003 color coded by speed ( $\text{cm s}^{-1}$ ). The location of the drifter on the 1st of each month is noted by black dots. Dashed line is 200 m depth contour.

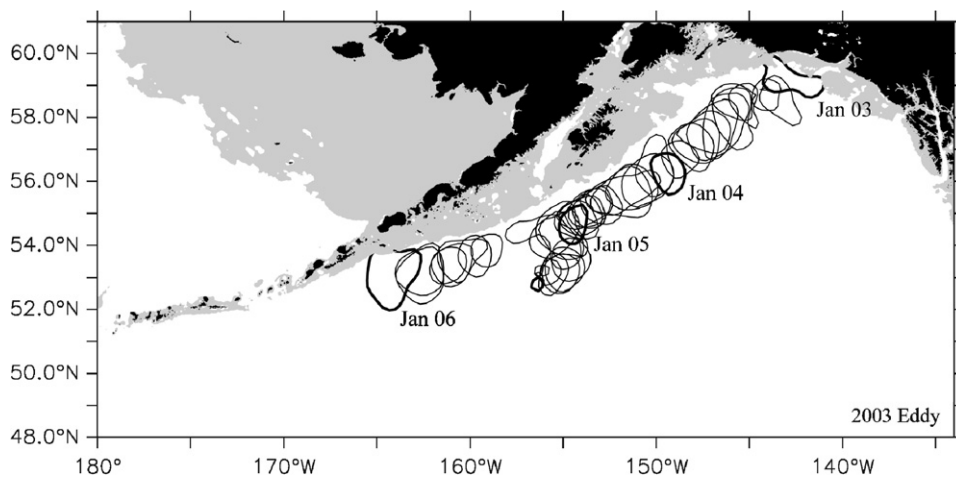


Fig. 8. SSHA 20 cm contours associated with the 2003 eddy plotted on the 15th of each month. January contours are bold.

(eddy center locations estimated from the 4 drifter circuits moved less than 30 km).

#### 4. 2003 eddy

The 2003 eddy was 1st observed in altimetry data in January 2003 offshore of Yakutat, Alaska (Fig. 8). This formation region (north of the 2001 eddy) was consistent with water properties of the core water observed in May 2003 (Ladd et al., 2005b). The eddy size was more consistent throughout its lifecycle than the 2001 eddy (Fig. 5). During their translation from the head of the gulf south-

westward past Kodiak Island, the 2001 eddy moved  $\sim 70\%$  faster than the 2003 eddy (Table 2).

The water properties of the 2003 eddy were sampled during May and September 2003 and May and October 2004. The eddy water properties during 2003 were described by Ladd et al. (2005b) and the details will not be discussed here. Instead, we concentrate on changes observed in the eddy between 2003 and 2004.

In May 2003, the water properties at the core of the eddy were distinct from the surrounding basin water in a density range of  $25.4\text{--}26.8 \text{ kg m}^{-3}$  (Fig. 9). Between May and September 2003, water

properties in the density range  $26.0\text{--}26.2\text{ kg m}^{-3}$  were the most changed (Fig. 9). Ladd et al. (2005b) speculated that mixing/exchange may have been enhanced in this density range by interactions with the shelf-break bathymetry. This density range also exhibited the largest decrease in nutrient concentration of the core water from May to September 2003 (see Section 6.1.1).

By May 2004, the eddy had survived a 2nd winter. The remnant of the winter mixed layer was approximately the same depth in May 2004 as in May 2003. However, this subsurface layer was colder in 2004 than in 2003 (by  $\sim 1.6\text{ }^{\circ}\text{C}$ ) suggesting that winter heat fluxes from the ocean to the atmosphere were stronger during the winter of 2003/2004 than 2002/2003. In fact, sea surface temperatures in this region estimated by NCEP averaged  $1\text{ }^{\circ}\text{C}$  colder in January–March 2004 than in the same months in 2003. Also National Data Buoy Center Station 46001 south of Kodiak Island ( $56.30^{\circ}\text{N}$ ,  $148.17^{\circ}\text{W}$ ) showed colder surface tem-

peratures during the winter of 2003/2004 than 2002/2003. While the winter mixing in 2003/2004 was approximately to the same depth as the year prior, mixing extended to greater densities. This resulted in the shallow part of the core waters being mixed away. In addition, as noted above, the denser part of the core water had also been partially eroded away by September 2003 by shelf-break interactions (Ladd et al., 2005b). Thus, by May 2004, the core water that remained was primarily in a density range of  $25.9\text{--}26.3\text{ kg m}^{-3}$  and was less distinct from the surrounding basin water.

At the end of September 2004, the eddy split into 2 sub-eddies. This split was apparent in both altimetry data and in a drifter trajectory (Fig. 10). The October 2004 hydrographic transect allowed an examination of the 2 sub-eddies just after the split (Fig. 11). The eddy signature of depressed isopycnals was stronger in the western sub-eddy. The center cast of the western sub-eddy remained warmer than the surrounding water in the density

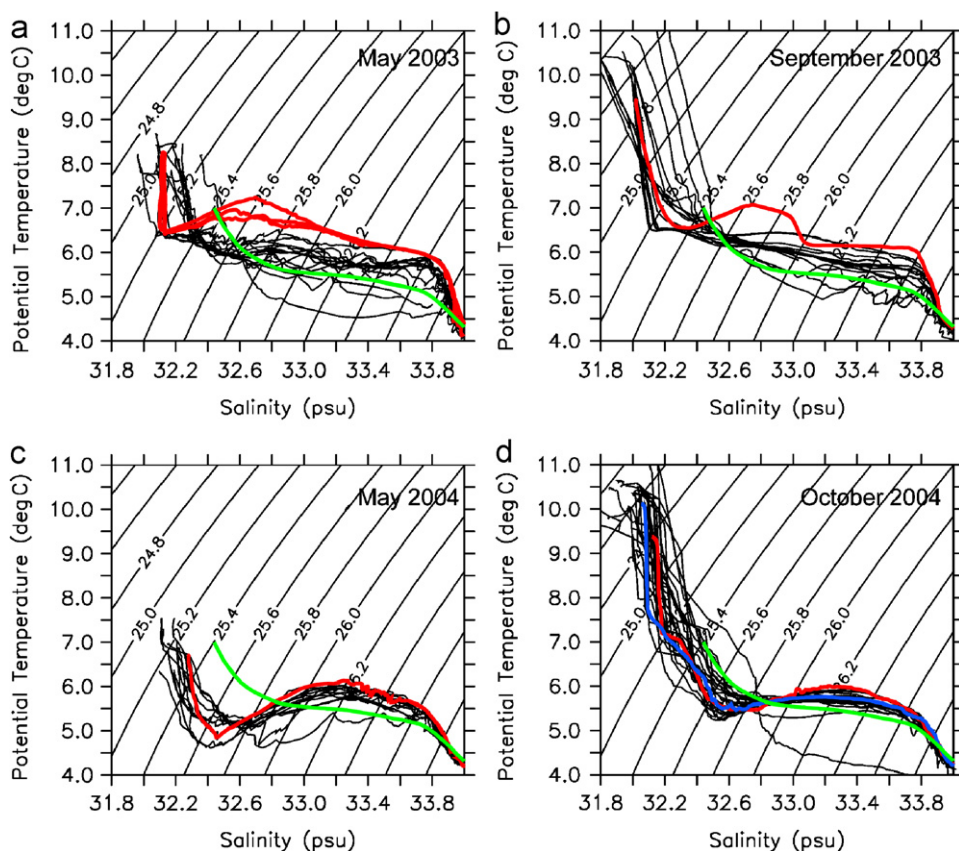


Fig. 9. Temperature/salinity relationship from surface to 600 m for the 4 transects across the 2003 eddy. Red lines represent cast nearest the center of the eddy. Green line is reference cast discussed in the text. In October 2004, the blue (red) line is cast near the center of the eastern (western) sub-eddy.

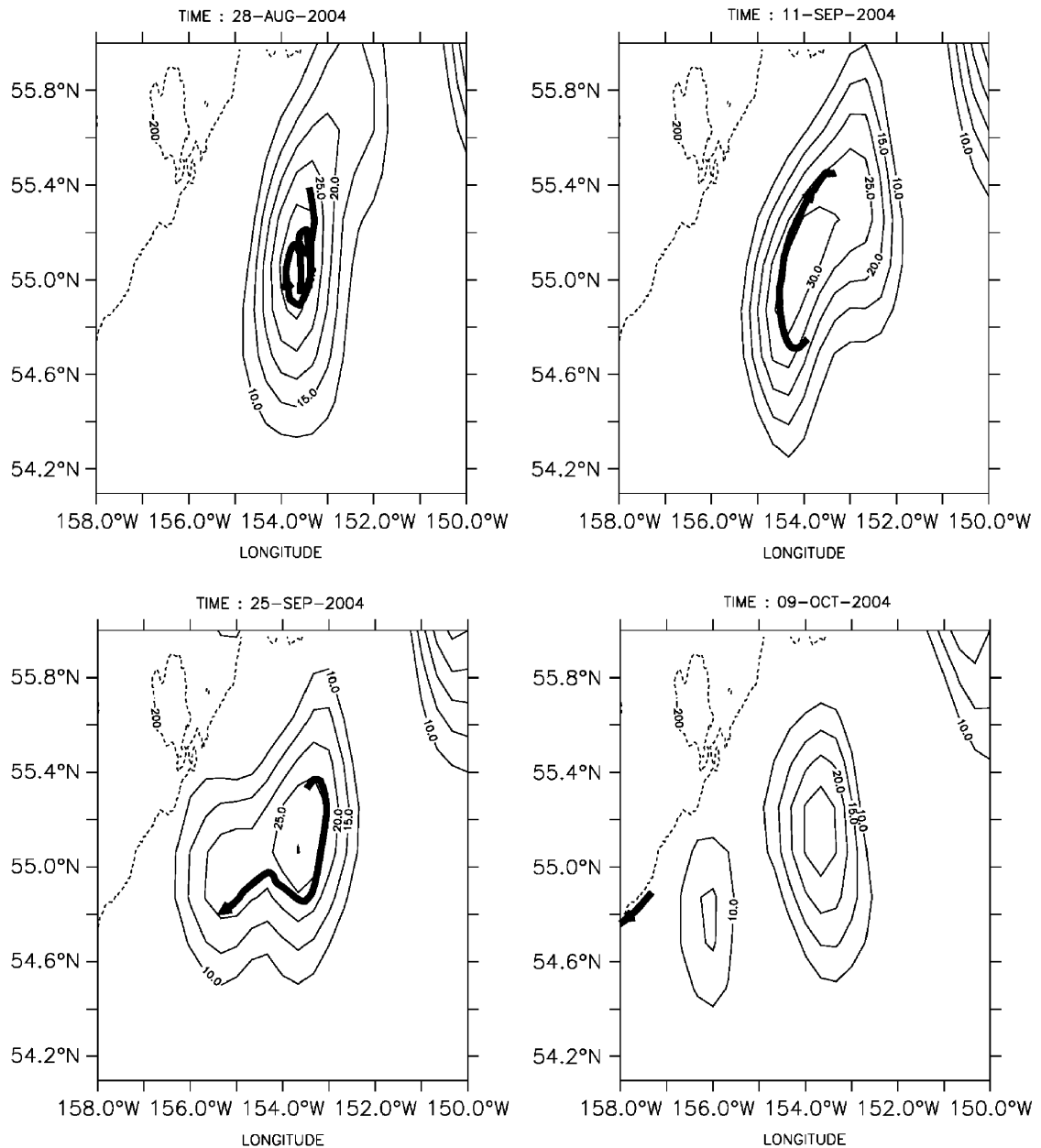


Fig. 10. SSHA contours (contour interval = 5 cm) every 14 days from 28 August 2004 until 9 October 2004. Bold line denotes drifter trajectory (no. 43 725) for the 10 days prior to the SSHA data with arrow showing direction. Dashed contour represents the 200 m isobath.

range  $26.0 < \sigma_{\theta} < 26.6 \text{ kg m}^{-3}$  (Fig. 9d). However, the center of the eastern sub-eddy (blue profile in Fig. 9d) was not distinguishable from the other casts on the transect. This lack of distinguishable core water in the eastern sub-eddy suggests that the core water mass remained with the western sub-eddy and did not split. Unfortunately, because of bad weather, the ship was not able to extend the transect past the western edge of the western sub-eddy to the shelf-break.

Favorite et al. (1976) identified water masses in the GOA that include the Ridge Domain water in the center of the Alaska Gyre and the Alaska Current water in the boundary current. Note that 1 cast on the October 2004 transect is much colder than the rest of the transect deeper than  $\sigma_{\theta} \sim 26.0 \text{ kg m}^{-3}$  (Fig. 9d). This cast is at the basin end of the transect and the water properties suggest that the cast sampled Ridge Domain water while the

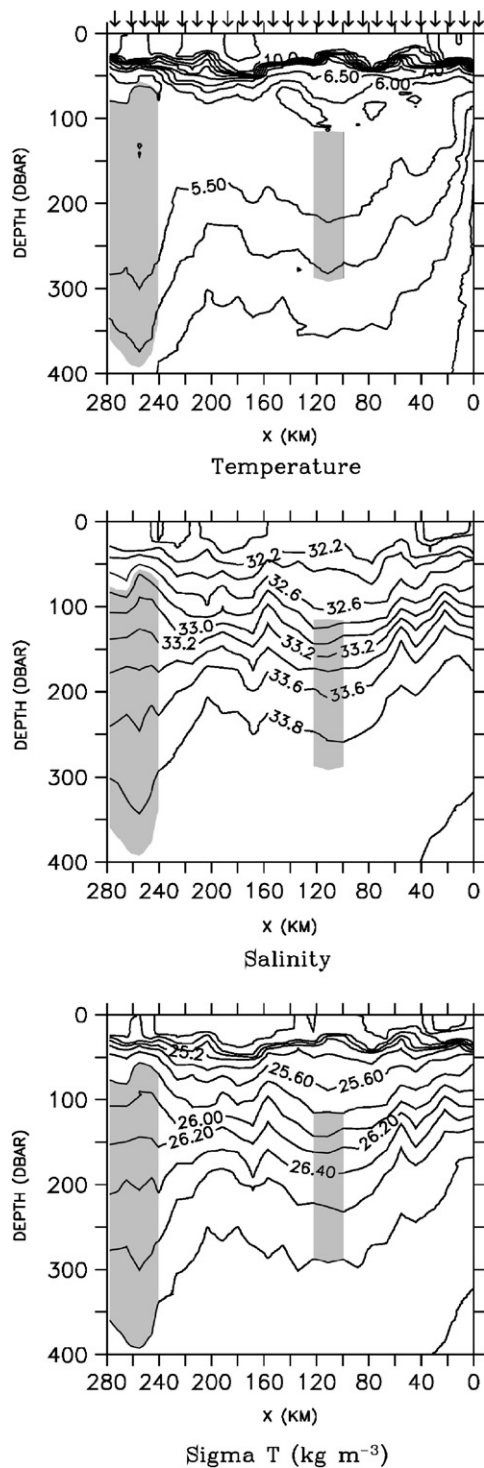


Fig. 11. Temperature ( $^{\circ}\text{C}$ ), salinity, and density ( $\sigma_t$ ,  $\text{kg m}^{-3}$ ) from the October 2004 transect across the 2003 eddy. The location of CTD casts is denoted by arrows in the top panel. Shading denotes the core water defined by  $25.8 \text{ kg m}^{-3} < \sigma_t < 26.8 \text{ kg m}^{-3}$  in the western and eastern sub-eddies.

rest of the transect sampled Alaska Current water. Ridge Domain water was also sampled in the July 2004 transect across the 2004 eddy (see Section 5 and Fig. 14).

After the split, the western sub-eddy weakened, until by January 2005, it was no longer visible in the altimetry data. The originally weaker eastern sub-eddy continued, splitting again in May 2005. One of the new sub-eddies continued along the shelf-break while the other moved southwestward away from the shelf (Fig. 8). As of January 2006, both sub-eddies were still in existence, a total lifetime for the 2003 eddy of at least 36 months. The history of the 2001 and 2003 eddies suggests that splitting of eddies is not uncommon.

### 5. 2004 eddy

Altimetry suggests that the 2004 eddy 1st appeared near the head of the gulf, away from the eastern boundary (Fig. 12). This is very close to the formation location of an eddy reported on by Crawford et al. (2000) (see their Fig. 2d) that formed in winter 1995. Prior to May 2004, there were multiple eddies in the region that appeared to be interacting so the origin of the 2004 eddy is complicated. At least 1 of these eddies appeared to originate on the shelf near Yakutat although it is unclear from the altimetry whether that eddy combined with others to form the 2004 eddy or disintegrated on its own. In any case, by the time the 2004 eddy was sampled in July, it was well formed and no longer interacting with other eddies. By May 2005, the 2004 eddy was no longer apparent in the altimetry data, suggesting a short lifetime (compared with the other eddies investigated here) of only 12 months. During 2004, the 2004 eddy had an average translation speed of  $3.3 \text{ km day}^{-1}$  and maximum SSHA averaging 30 cm, within the range of the other eddies (Table 2).

The May 2004 transect missed the eddy center by more than 50 km. However, a drifter deployed during the May transect (43 720) provided data that directed the July transect to within 8 km of the eddy center. Since no drifters were in the eddy in October (Table 1), we do not have an accurate estimate of the eddy center location during the October transect. However, water properties suggest that the transect came close to the eddy center. Thus, we show data from both the July and the October transects (Figs. 13 and 14). The July transect consisted of 21 CTD casts over a distance of

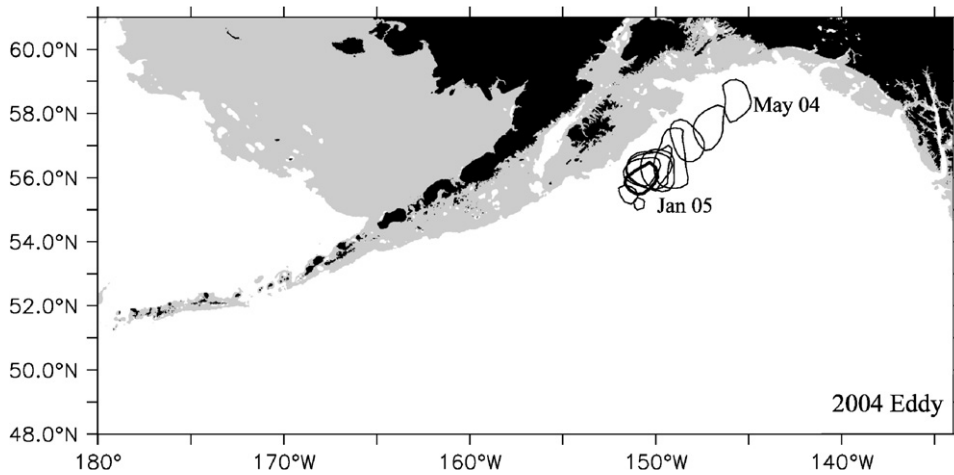


Fig. 12. SSHA 20cm contours associated with the 2004 eddy plotted on the 15th of each month.

~230 km while the October transect consisted of 19 casts over a distance of ~225 km. At the center of the transects, a subsurface temperature maximum ( $T > 6^\circ\text{C}$ ) was associated with the core water of the eddy and salinities were fresher than water at the same depth outside the eddy throughout the water column (Figs. 13 and 14). At 175 m depth, the temperature at the center of the eddy was over  $2.5^\circ\text{C}$  warmer in July and  $1.5^\circ\text{C}$  warmer in October than water at the same depth outside the eddy. The maximum salinity anomaly was 1.15 in July and 0.8 in October and was observed at ~125 m depth.

The temperature/salinity relationship illustrates the unique water properties of the eddy core water compared to the CTD casts taken farther from the eddy center (Fig. 14). In the density range  $25.8 < \sigma_\theta < 26.8 \text{ kg m}^{-3}$ , the water properties in the center of the eddy are clearly different from the water properties of the other casts. Note that the radius of the distinct core water was particularly large (~70 km in July 2004; ~35 km in October 2004). For comparison, the radius of the core water for the 2003 eddy sampled in May 2003 was between 19 and 38 km (Ladd et al., 2005b). This may be due to the later formation of the 2004 eddy (May), suggesting that it was sampled when it was younger and had not lived through a full winter mixing season.

While the water properties of the eddy core water did not change dramatically between July and October, the properties of the surrounding water changed significantly. Temperatures at densities greater than  $\sigma_\theta = 26.0 \text{ kg m}^{-3}$  were colder in July ( $4\text{--}5.5^\circ\text{C}$ ) than in October ( $> 5^\circ\text{C}$ ). The differences

in the waters surrounding the 2004 eddy indicate that the eddy was surrounded by Ridge Domain water (Favorite et al., 1976; Musgrave et al., 1992) in July and Alaska Current water (Aydin et al., 1998; Musgrave et al., 1992) in October. Since Ridge Domain water (also called Alaskan Gyre water by Aydin et al., 1998) defines the center of the Alaskan Gyre, these observations indicate that the eddy may be responsible for pulling Ridge Domain water closer to the shelf break than it would be otherwise.

## 6. Heat, salinity, and nutrient anomalies

Altimetry data and water properties suggest that northern GOA eddies form on or near the shelf in the eastern GOA, enclosing shelf water in their interior and advecting that shelf water into the basin. With the hydrographic data collected on transects crossing the center of the eddies, we can estimate the heat, salt, and nutrient anomalies contained in the core waters.

Following Joyce et al. (1981) and van Ballegooyen et al. (1994), assuming axial symmetry, the heat anomaly ( $\text{HA}_\sigma$ ) contained on each discrete  $\sigma_\theta$  density layer can be calculated by

$$\text{HA}_\sigma = \int_0^{2\pi} \int_0^{R_\sigma} \rho_\sigma c_p h_\sigma(r) [T_\sigma(r) - T_\sigma(\text{ref})] r \, dr \, d\theta,$$

where  $\rho_\sigma$  is the in situ density ( $\text{kg m}^{-3}$ ) within the  $\sigma_\theta$  layer;  $c_p$  the specific heat capacity ( $\text{J kg}^{-1} \text{ }^\circ\text{C}^{-1}$ ) within the  $\sigma_\theta$  layer;  $h_\sigma(r)$  the thickness (m) of the  $\sigma_\theta$  layer;  $r$  the radial distance (m) from the center of the eddy;  $T_\sigma(r)$  the in situ temperature ( $^\circ\text{C}$ ) within the  $\sigma_\theta$

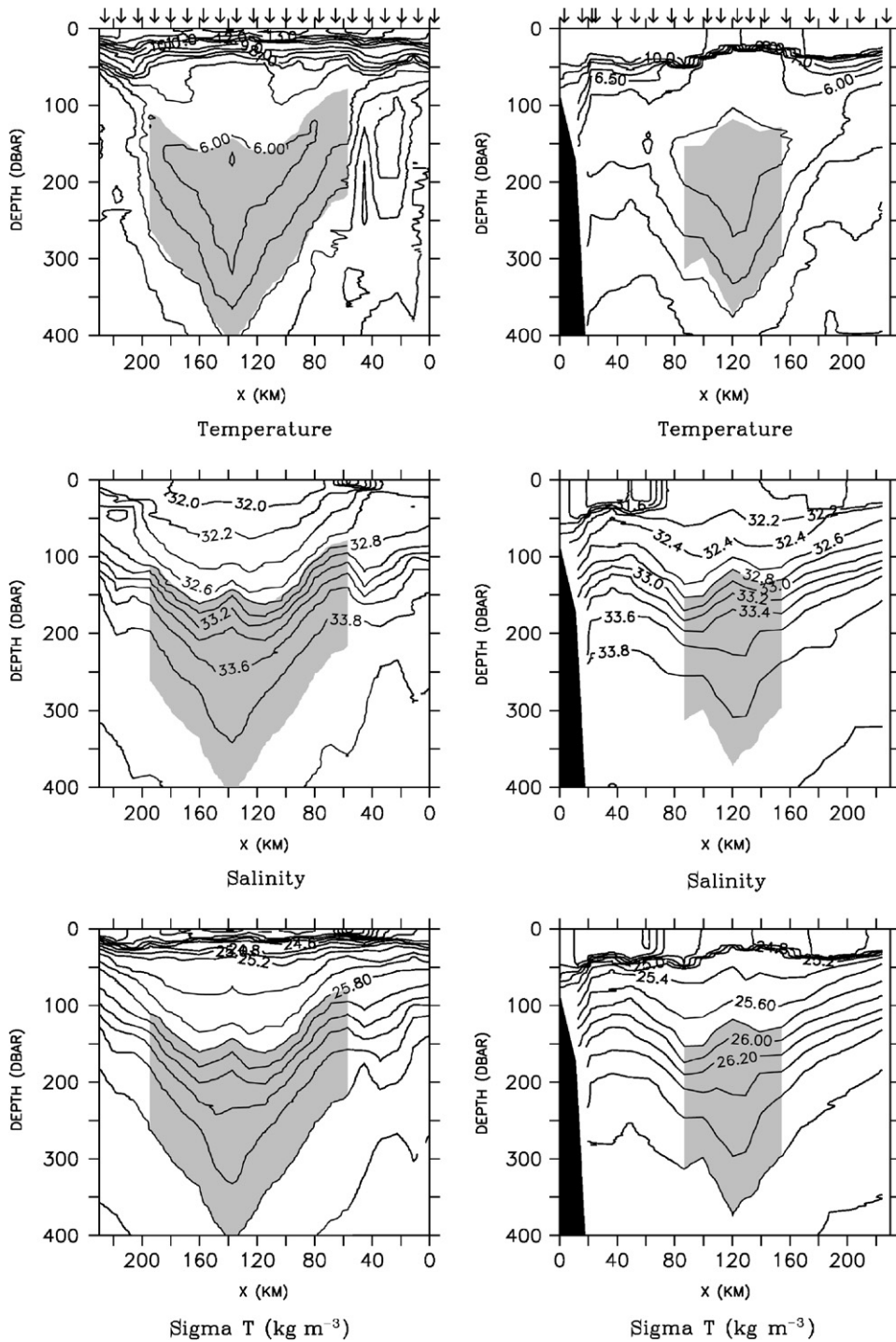


Fig. 13. Temperature ( $^{\circ}\text{C}$ ), salinity, and density ( $\sigma_t$ ,  $\text{kg m}^{-3}$ ) from the July 2004 (left) and the October 2004 (right) transects across the 2004 eddy. The location of CTD casts is denoted by arrows in the top panel. Shading denotes the core water defined by  $25.8 \text{ kg m}^{-3} < \sigma_t < 26.8 \text{ kg m}^{-3}$ ; casts 6–18 (July) and casts 9–15 (October).

layer;  $T_{\sigma}(\text{ref})$  the in situ temperature ( $^{\circ}\text{C}$ ) within the  $\sigma_{\theta}$  layer at the reference station (see below);  $R_{\sigma}$  the estimated radius (m) of the core water.

A standard radius of  $R_{\sigma} = 50 \text{ km}$  was used to facilitate comparisons between transects. However, because the 2004 eddy was observed to have a larger

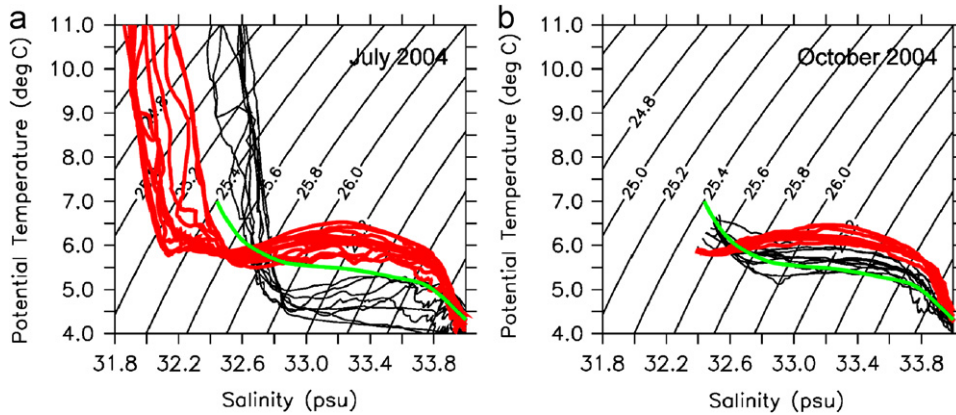


Fig. 14. Temperature/salinity relationship from transects across the 2004 eddy (a) surface to 600m from July 2004 and (b)  $25.5 < \sigma_\theta < 27.0 \text{ kg m}^{-3}$  from October 2004. Red lines denote casts 6–18 in July and 9–15 in October (core water). Green line is reference cast discussed in the text.

radius, anomalies were also calculated using  $R_\sigma = 60 \text{ km}$  to illustrate the influence of the choice of radius. Because none of the transects had a cast at exactly 50 km from the center cast, linear interpolation was used to simulate a cast at 50 km from the center. Because all of the transects were close to the shelf-break on 1 end, the integrated anomalies were calculated using only the half of the transect from the eddy center toward the basin so as to avoid influences due to interaction with the shelf-break.

Similarly, the salt anomaly ( $SA_\sigma$ ) and nutrient (nitrate and silicic acid) anomaly ( $NA_\sigma$ ) were calculated as

$$SA_\sigma = \int_0^{2\pi} \int_0^{R_\sigma} 0.001 \rho_\sigma h_\sigma(r) [S_\sigma(r) - S_\sigma(\text{ref})] r dr d\theta,$$

$$NA_\sigma = \int_0^{2\pi} \int_0^{R_\sigma} 1000 h_\sigma(r) [N_\sigma(r) - N_\sigma(\text{ref})] r dr d\theta,$$

where  $S_\sigma(r)$  is salinity and  $N_\sigma(r)$  is either nitrate or silicic acid ( $\mu\text{mol l}^{-1}$ ) within the  $\sigma_\theta$  layer. The factor of 0.001 converts salinity to the mass of salt per unit mass of seawater. The factor of 1000 converts liters to  $\text{m}^3$ .

The reference temperature and salinity profiles were calculated by averaging (on density surfaces) data from casts at the basin end of 3 transects (KM0309, KM0313, and HX287). This average profile was then smoothed (with a smoothing scale of  $\sigma_\theta \sim 0.35 \text{ kg m}^{-3}$ ) to remove small-scale variations. The reference nutrient profile was the average of the profiles at the basin ends of KM0309 and KM0313. The casts used to create the reference

profile were chosen because they were far from any SSH anomalies (based on altimetry data) that might indicate eddies, they were far from the slope, and they were in the same general region of the gulf (north of  $\sim 56.5^\circ \text{N}$ ). Thus, the reference profile should be representative of the water properties in this region of the Gulf of Alaska basin. The resulting reference profile exhibits water properties similar to the Alaska Current water mass described by Musgrave et al. (1992) and Aydin et al. (1998). Temperatures on an isopycnal were warmer than the reference in 2003 while they were cooler than the reference in July 2004 (compare Figs. 9 and 14). Thus, while the use of a single reference profile allows a comparison of anomalies over time, it may misrepresent the anomaly as referenced to the contemporary water column structure.

To obtain the total heat and salt anomalies associated with the eddy, the anomalies in each discrete  $\sigma_\theta$  layer were integrated over 2 different density ranges (Table 3). The larger density range,  $25.5 < \sigma_\theta < 27.0 \text{ kg m}^{-3}$ , was used to encompass the entire anomalous water mass of the 2003 eddy in May 2003. However, as discussed previously the core waters contracted in density space over time resulting in negative anomalies above and below the core in the later transects. Thus, anomalies calculated over a smaller density range,  $26.0 < \sigma_\theta < 26.6 \text{ kg m}^{-3}$ , allow analysis of the changes in the main core over time. Nutrient anomalies were calculated over the density range  $25.5 < \sigma_\theta < 26.4 \text{ kg m}^{-3}$  as the differences between observations from the eddy center and the reference cast were significant in this range.

Table 3  
Excess heat, salt and nutrient content of eddies in subsurface core waters

Density range ( $\sigma_\theta$ )	Heat Anomaly ( $10^{18}$ J)		Salinity Anomaly ( $10^{10}$ kg)		Nitrate Anomaly ( $10^9$ moles)	Silicic acid Anomaly ( $10^9$ moles)
	25.5–27.0	26.0–26.6	25.5–27.0	26.0–26.6		
<i>2003 Eddy</i>						
May 2003 (KM0309)	5.7	3.2	21.1	12.2	1.2	3.6
September 2003 (KM0313)	2.9	2.1	10.5	7.9	2.1	4.0
May 2004 (HX284; cross-shelf)	−0.9	1.4	−3.9	5.3		
May 2004 (HX284; along-shelf)	−0.4 <sup>a</sup>	1.5	−1.6 <sup>a</sup>	5.7		
October 2004 (EW0409)	0.5	0.9	1.3	3.3		
<i>2004 Eddy</i>						
July 2004 (HX287)	2.4	1.8	8.4	7.0		
	3.0 <sup>b</sup>	2.4 <sup>b</sup>	10.7 <sup>b</sup>	9.2 <sup>b</sup>		
October 2004 (EW0409)	1.8	1.7	6.2	6.5		
	1.6 <sup>b</sup>	2.0 <sup>b</sup>	5.6 <sup>b</sup>	7.7 <sup>b</sup>		

<sup>a</sup>Density range of 25.5–26.7 used because of inadequate sampling below 500 m.

<sup>b</sup>Radius of 60 km used for anomaly calculation.

Calculating the anomalies on potential density surfaces as opposed to pressure surfaces ensures that the anomalies are solely due to the transport of anomalous water masses and not due to changes in the vertical position of density surfaces associated with the available potential energy of the eddy.

## 6.1. Results

Heat and salinity anomalies for the 2003 and 2004 eddies were calculated for each transect that sampled within 20 km of the eddy center (Table 3). Nitrate and silicic acid anomalies were only available in 2003 for the 2003 eddy.

### 6.1.1. 2003 eddy

In May 2003, the heat anomaly at the center of the 2003 eddy had a bimodal structure with maxima at  $\sigma_\theta = 25.8$  and  $26.7 \text{ kg m}^{-3}$  (Fig. 15a). The bimodal structure was not due to the structure of the reference profile. Both maxima had a contribution from both  $T_\sigma(r) - T_\sigma(\text{ref})$  and  $h_\sigma(r)$ . However,  $T_\sigma(r) - T_\sigma(\text{ref})$  contributed more to the maxima in the shallower layer ( $\sigma_\theta = 25.8 \text{ kg m}^{-3}$ ) while  $h_\sigma(r)$  had a higher contribution in the deeper layer ( $\sigma_\theta = 26.7 \text{ kg m}^{-3}$ ).

A positive heat anomaly on isopycnals implies a positive salinity anomaly due to the opposing influences of temperature and salinity on density. Thus, these eddies carry both anomalous heat and

anomalous salinity into the basin. The salinity anomaly had a similar bimodal structure (not shown). The shallower maximum (at  $\sigma_\theta = 25.8 \text{ kg m}^{-3}$ ) was tightly constrained to the center of the eddy, dropping off rapidly more than 19 km away from the center (the casts were separated by  $\sim 19$  km). The deeper maximum was much more broadly distributed with positive anomalies to the end of the transect. Comparison of the reference cast with the May 2003 eddy casts on the temperature–salinity plot (Fig. 9a) shows that, with the exception of 3 casts at the edges of the eddy, the casts within the eddy were warmer on an isopycnal than the reference cast on the layers  $\sim 25.6 < \sigma_\theta < \sim 26.9 \text{ kg m}^{-3}$ . Shallower than  $\sigma_\theta \sim 25.4 \text{ kg m}^{-3}$ , the water in the center of the eddy was colder and fresher than the surrounding water.

In September 2003, the bimodal structure was still apparent (Figs. 9b and 15b) but the anomaly was not as broadly distributed as in May. In fact, the total HA calculated over  $25.5 < \sigma_\theta < 27.0 \text{ kg m}^{-3}$  dropped to  $\sim 50\%$  of that calculated for May (Table 3). Calculating the HA over the  $26.0 < \sigma_\theta < 26.6 \text{ kg m}^{-3}$  density range results in a reduction of 35% between May and September. Salinity anomalies show similar reductions.

As noted previously, the shallower layers of the eddy were colder in May 2004 than in 2003. At the center of the eddy in 2004, the surface waters down to  $\sigma_\theta \sim 25.9 \text{ kg m}^{-3}$  were colder than the reference



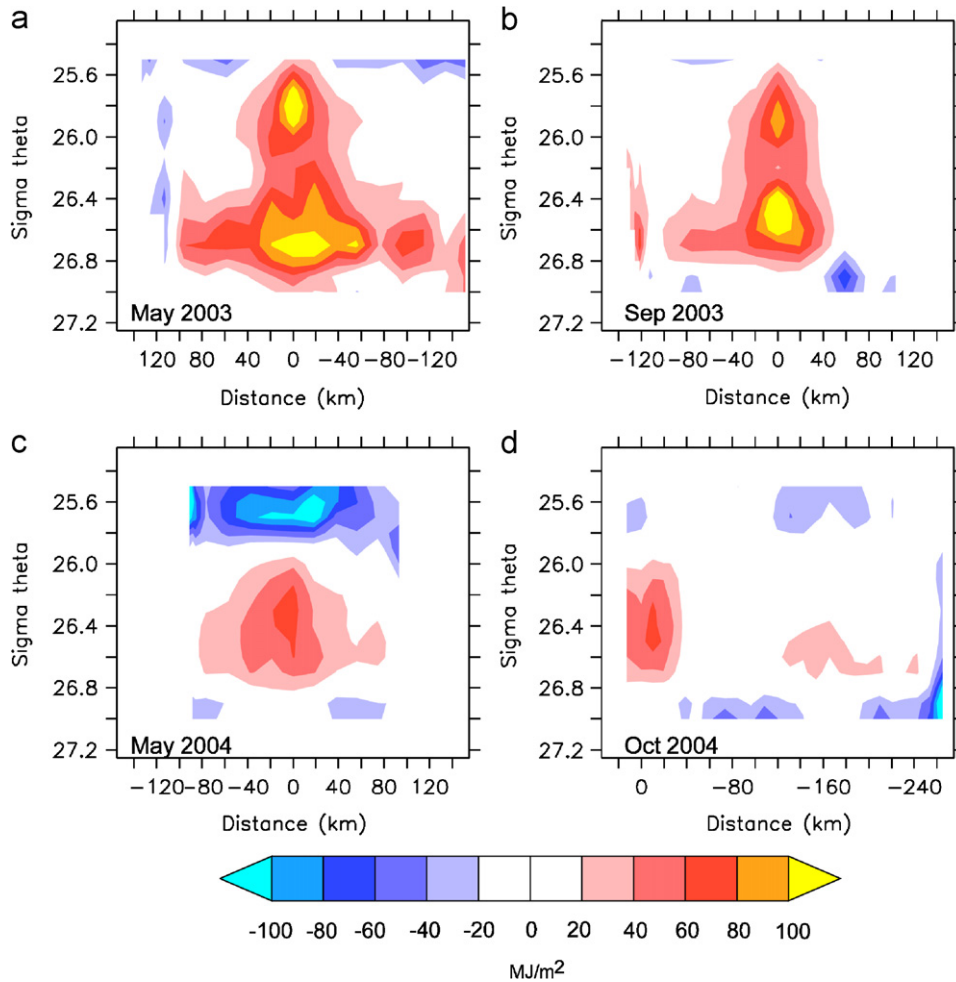


Fig. 15. Heat anomaly per unit area ( $\text{MJ m}^{-2}$ ;  $\text{MJ} = 10^6 \text{J}$ ) in the 2003 eddy in (a) May 2003; (b) September 2003; (c) May 2004; and (d) October 2004. The horizontal axis is standardized to display the center of the eddy at 0 km in the center of the plots. Note that in (d), the center of the western sub-eddy at 0 km is shown near the left of the plot in order to show the entire transect.

station (Fig. 9c). The maximum heat anomaly occurred in the layer  $\sigma_\theta \sim 26.4 \text{ kg m}^{-3}$  and the bimodal structure was no longer in evidence (Fig. 15c). The HA and SA calculated over the larger density range (25.5–27.0) became negative in May 2004 indicating that the eddy contained a heat and salinity deficit compared to the reference cast. However, calculated over the tighter core densities (26.0–26.6), HA and SA decreased from September 2003 to May 2004 to roughly half that originally calculated for May 2003.

In the same way, anomalies of other chemical constituents (nutrients) can be calculated. In order to calculate the nitrate and silicic acid anomalies, we first linearly interpolate the data in depth so that nitrate and silicic acid are resolved on all of the density layers. To illustrate changes in

nutrient concentrations within the eddy (not confounded with changes in layer thickness), Fig. 16 shows  $N_\sigma(r) - N_\sigma(\text{ref})$  without multiplying by  $h_\sigma(r)$ . However, Table 3 includes the entire integrated anomaly.

Both nitrate and silicic acid exhibited positive anomalies at the center of the 2003 eddy with respect to the reference profile (Fig. 16, Table 3). This was consistent with data from the eastern Gulf of Alaska shelf that exhibited excess nitrate with respect to salinity (see Fig. 8 from Ladd et al., 2005b). In May 2003, the maximum nutrient anomalies were at densities shallower than  $\sigma_\theta \sim 26.4 \text{ kg m}^{-3}$  and tightly confined to the center of the eddy. By September 2003, the positive anomalies had spread farther from the center of the eddy.

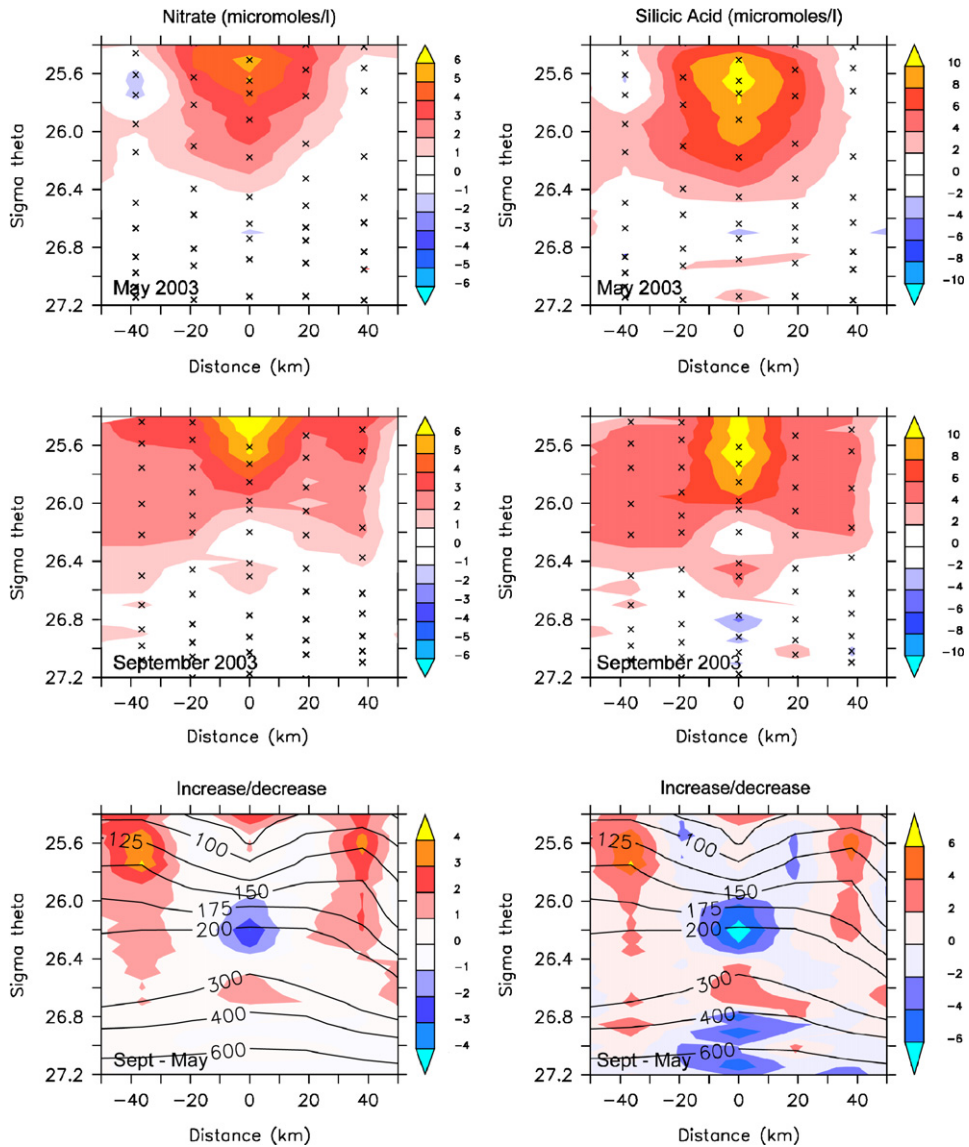


Fig. 16. Nitrate (left) and silicic acid (right) anomalies ( $\mu\text{M}$ ) in the 2003 eddy in May 2003 (top) and September 2003 (middle) and differences (September—May; bottom). Location of bottle data in  $\sigma_\theta$  space is denoted by  $x$ 's. The horizontal axis is standardized to display the center of the eddy at 0 km in the center of the plots. Black contours in the difference plots (bottom) denote the depth (m) of the  $\sigma_\theta$  surfaces in September 2003.

The difference in nutrient anomalies from May to September (Fig. 16, bottom panels) showed considerable horizontal and vertical structure. Horizontal variations could be the result of isopycnal mixing. In the density range  $\sim 26.0 < \sigma_\theta < \sim 26.4 \text{ kg m}^{-3}$ , nutrient content at the center of the eddy decreased from May to September while nutrient content farther from the center ( $\sim 40 \text{ km}$  from the center) increased. Such reversals in sign along isopycnals (e.g. between 0 and 40 km along  $\sigma_\theta = 26.2 \text{ kg m}^{-3}$ ) strongly suggest mixing or ex-

change along isopycnals, a mechanism that also affected temperature and salinity profiles (see Section 4; also Ladd et al., 2005b). However, the increase in nitrate and silicate  $\sim 40 \text{ km}$  from the center (integrated around the ring) was greater than the decrease near the center. Thus, this mechanism cannot account for the entire change from May to September.

Vertical variations could be the result of diapycnal mixing, especially at the edges of the eddy where the sloping isopycnals are compressed. Alone, this

mechanism would produce vertical reversals in the sign of the seasonal change in nutrients. Although this result was not observed, reversals in the sign may be masked by concurrent processes (e.g. isopycnal mixing, remineralization), and thus, this mechanism cannot be discounted.

Unlike HA and SA, both nitrate and silicic acid anomalies increased from May to September 2003 (Table 3, integrating over the entire 50 km radius accounts for any mixing within that radius). Remineralization of nitrate and dissolution of opal are likely mechanisms for explaining these increases, especially at the edge of the eddy.

Oceanic remineralization (i.e. the biologically mediated transformation of organic matter into inorganic forms, and the concomitant consumption of oxygen) replenishes inorganic nutrients in accordance with the Redfield ratio:  $-O_{2\ 170}:C_{org\ 117}:N_{16}:P_1$  (Anderson and Sarmiento, 1994). Just below the euphotic zone (in the density range  $\sigma_\theta = 25.5\text{--}26.4\text{ kg m}^{-3}$ ), nitrate and phosphate anomalies averaged over 50 km from the center of the eddy increased by 0.9 and  $0.06\ \mu\text{mol l}^{-1}$ , respectively from May to September, consistent with the Redfield ratio. (Nitrate is shown in the left panels of Fig. 16; phosphate is not shown.) Although oxygen was not measured, these nutrient changes equate to an oxygen utilization rate (OUR) of  $26\ \mu\text{mol kg}^{-1}\text{ yr}^{-1}$ , a rate that is 2–3 times greater than measurements of OUR in the subarctic Pacific ( $15\ \mu\text{mol kg}^{-1}\text{ yr}^{-1}$  by Warner et al., 1996; and  $10\ \mu\text{mol kg}^{-1}\text{ yr}^{-1}$  by Feely et al., 2004 at 150 m).

Higher remineralization rates, especially at the perimeter of the eddy, were likely the result of enhanced primary and secondary production in the eddy that facilitated the vertical flux of nutrients. Mesoscale eddies in the GOA are known to be dominated by diatoms in spring, and to have higher, shelf-like, concentrations of chlorophyll (Crawford et al., 2005). Indeed, in 2003, SeaWiFS imagery revealed that in April, the eddy core had shelf-like concentrations of chlorophyll, and in May, the eddy had a ring of high chlorophyll extending 35–50 km from its center (Ladd et al., 2005b; see their Fig. 9). Likewise, zooplankton are relatively abundant in eddy ecosystems (Batten and Crawford, 2005; Mackas and Galbraith, 2002; Mackas et al., 2005), and may contribute to the rapid remineralization of nutrients in the water column (Kiørboe, 2003; Smetacek, 1980; Viitasalo et al., 1999).

About 50% of biogenic silica is thought to dissolve rapidly in the upper 100 m (Nelson et al.,

1995) with the specific dissolution rate dependent on physical characteristics of the ocean (temperature, pH and electrolyte composition) as well as the characteristics of the silica (surface area, impurity content and age) (Ragueneau et al., 2000; Van Cappellen et al., 2002). Based on the seasonal change in dissolved silicic acid in the density range of  $\sigma_\theta = 25.5\text{--}26.4\text{ kg m}^{-3}$  and from 0 to 50 km from the eddy center, the dissolution rate is estimated to be  $0.17\text{ mol Si m}^{-2}\text{ yr}^{-1}$ , about 3 times lower than the global mean calculated for the upper water column (Van Cappellen et al., 2002). However, the temperature dependence ( $Q_{10}$ ) of biogenic silica dissolution is a factor of  $\sim 2.3$  per  $10^\circ\text{C}$  (Bidle et al., 2002), and water temperatures in the core of the eddy were about  $7\text{--}9^\circ\text{C}$  colder than upper waters in the North Pacific. When corrected to upper water temperatures, the dissolution rate estimated in the eddy core water is similar to the global mean. Other factors that might contribute to lower dissolution rates include higher concentrations of aluminum in these shelf-derived waters, a trace metal known to slow dissolution when incorporated into diatom frustules (Van Cappellen et al., 2002), and the lower surface area of sinking particles at these depths (100–200 m, Pilskaln et al., 1998; Walsh and Gardner, 1992).

#### 6.1.2. 2004 eddy

The HA and SA calculated for the 2004 eddy were roughly half those calculated for the 2003 eddy in May of its natal year. However, as noted previously, the 2004 eddy had a larger radius than the 2003 eddy. Therefore, HA and SA calculations were extended to a radius of 60 km resulting in an increase in anomalies of 20–30% from anomalies calculated for a radius of 50 km (Table 3).

Differences between the HA and SA calculated from the 2 HX284 transects occupied in May 2004 can give some indication of the level of uncertainty in these calculations. Two possible sources of error are confounded in these 2 transects: effects of horizontal resolution and of distance from the center of the eddy. The along-shelf transect had higher horizontal resolution with casts every 9–10 km. (Except for HX284 along-shelf transect and the EW0409 cruise ( $\sim 10$  km spacing), all of the other transects had spacing of  $\sim 19$  km between casts.) In addition, the along-shelf transect sampled closer to the center of the eddy by  $\sim 9$  km as determined from drifter data. The HA and SA

calculated for the 2 transects differed by less than 10%, suggesting uncertainties of that magnitude.

## 7. Discussion

The 3 eddies that were examined near the shelf-break northeast of Kodiak Island over 3 different years had 3 different formation regions. However, their pathways were similar. While eddies formed in the southern GOA (Haida and Sitka eddies) have fixed formation locations and more variable pathways, northern GOA eddies have variable formation regions (which may include the Sitka formation region) and more fixed pathways.

Water properties in the 2003 and 2004 eddies were significantly different from each other. The 2004 eddy did not exhibit a temperature maximum at the shallow densities ( $\sigma_\theta \sim 25.6 \text{ kg m}^{-3}$ ) of the 2003 eddy. This core in the 2003 eddy was shown by Ladd et al., 2005b to be derived from shelf water near Yakutat. The absence of this temperature maximum at  $\sigma_\theta \sim 25.6 \text{ kg m}^{-3}$  in the 2004 eddy is probably due to the fact that its formation region is farther from the shelf-break. The fact that the winter of 2003/2004 was colder than 2002/2003 resulting in a denser mixed layer may also have contributed to the lack of a temperature maximum at  $\sigma_\theta \sim 25.6 \text{ kg m}^{-3}$  in the 2004 eddy. Deeper than  $\sigma_\theta \sim 26.0 \text{ kg m}^{-3}$ , the water properties of the 2 eddies were similar in their initial years. The most dramatic difference between the 2003 and the 2004 eddies is the difference in the radius of their core waters (<40 km for 2003 eddy (May); ~70 km for 2004 eddy (July)). Of course with only 2 examples, we cannot say whether these differences are typical of differences between eddies formed in the 2 different regions. However, these observations illustrate that eddies in the northern GOA have variable formation regions and water properties.

Exchange between eddy formation regions and the basin can result from eddies trapping shelf water in their interiors and transporting it seaward. By measuring the same eddy multiple times throughout its journey, we can estimate the timing and magnitude of exchange between the shelf-derived eddy core water and the basin water. Altimetry data suggests that the 2003 eddy formed near Yakutat in January 2003. The surface layer (shallower than  $\sigma_\theta = 26.0 \text{ kg m}^{-3}$ ) was likely trapped inside the forming eddy and transported into the basin along with the core water. However, surface mixing during the winter erased any unique signature in

the winter mixed layer. In addition, Ekman transport would have allowed the Ekman layer to partially exchange with basin waters, not remaining completely trapped within the eddy (Mackas et al., 2005). Thus, between formation in January and our 1st in situ observations in May, some exchange between the eddy and the surrounding basin water had already occurred. In May 2003, the eddy contained  $3.2 \times 10^{18} \text{ J}$  of heat anomaly and  $12.2 \times 10^{10} \text{ kg}$  of salinity anomaly in the  $26.0 < \sigma_\theta < 26.6 \text{ kg m}^{-3}$  layer (Table 3). The heat and salinity anomalies recorded in the 2003 eddy declined over time with less than half the original (May 2003) anomalies still present in the core water a year later. While the 2004 eddy had a larger radius than the 2003 eddy, it contained smaller heat and salinity anomalies (even when calculated over a larger radius) possibly because of its offshore formation region.

Comparison with net ocean/atmosphere heat flux supplies a context for the anomalous heat content of the eddy core water. From May to September 2003, the eddy traveled ~140 km. Assuming a 50 km radius, the eddy moved through a swath with area ~14 000 km<sup>2</sup>. Over this time, the core lost  $1.1\text{--}2.8 \times 10^{18} \text{ J}$  of heat to the surrounding waters resulting in a heat loss per unit area of ~7.6–19.3 W m<sup>-2</sup>. For the months May–September, the average climatological net heat flux (shortwave, longwave, sensible, and latent) in this region from the NCEP reanalysis (Kalnay et al., 1996) is ~100 W m<sup>-2</sup> from the atmosphere to the ocean while the average annual net heat flux is ~15 W m<sup>-2</sup> from the ocean to the atmosphere. Thus, these eddies contribute significantly to the heat balance of the region through which they travel.

Crawford (2005) calculated the heat and freshwater transport by Haida eddies in the eastern GOA (~49°N–52°N; south of our area of interest) using anomalies with depth (as opposed to density). They found that Haida eddies transport  $10^{19}\text{--}10^{20} \text{ J}$  of heat and  $50 \text{ km}^3$  of freshwater seaward. However, their anomalies include the influence of changes in depth of isopycnals due to the dynamics of the eddy and are not comparable to the anomalies calculated here.

Our result, that eddies carry anomalous heat, salt, nitrate and silicic acid seaward, is counterintuitive as the shelf of the GOA is considered to be fresh and nitrate-poor relative to the basin. However, Ladd et al. (2005b) showed data from the eastern GOA shelf that illustrated that at the density of the eddy

core waters, the shelf waters were higher in salinity and nitrate (on a density surface) than the corresponding basin waters (see their Figs. 7 and 8). Aydin et al. (1998) also observed numerous eddies along the eastern boundary of the Gulf of Alaska with high salinity and warm temperatures relative to the basin, particularly on  $\sigma_\theta = 26.0 \text{ kg m}^{-3}$ . Aydin et al. (2004) found that the eastern boundary waters are warm and salty relative to the basin due to isopycnal mixing processes along the subarctic front.

The signature of fresher water on the shelf due to coastal runoff is generally confined to a shallow layer very close to the coast (i.e. Weingartner et al., 2005). The shallow layer within an eddy would be subject to wind forcing and would not remain trapped within the eddy for long, especially during the winter. Thus, an eddy may transport some fresher water seaward in its surface layers initially, but that water would not remain with the eddy for very long.

Our study of 3 large, persistent eddies that translated southwestward along the shelf-break seaward of Kodiak Island in 2002, 2003, and 2004 needs to be put in the context of a longer timeframe. Eddies in this region appear to be important to the ecosystem of the GOA, influencing distributions of phytoplankton and foraging behavior of fur seals. Thus, it is important to determine whether this period, with an annual occurrence of eddies in the region, is unique. An examination of the satellite altimetry record from 1993 to 2004 suggests that eddies may have been more frequent and persistent in the years since ~1999. This result implies that the GLOBEC years (2001–2004) may have been biased toward higher cross-shelf exchange. No new eddies were observed in the region near Kodiak Island in the springs of 2005 and 2006.

### Acknowledgments

We are grateful to the officers and crews of the R.V. *Maurice Ewing*, the R.V. *Kilo Moana*, and the R.V. *Alpha Helix* for their hard work in obtaining data in the eddies. Zachary Chen was very helpful in analyzing the altimetry data. Sigrid Salo provided SeaWiFS imagery. Three reviewers provided insightful comments that led to improvements in the paper. SeaWiFS level 1A data were obtained from the Goddard Earth Sciences Distributed Active Archive Center, which is under the auspices of the National Aeronautics and Space Administration.

Files were processed using SeaDAS (SeaWiFS Data Analysis System) which is maintained and distributed by the Goddard Space Flight Center. Use of this data is in accord with the SeaWiFS Research Data Use Terms and Conditions Agreement. The “ref merged” altimeter products were produced by Ssalto/Duacs and distributed by Aviso with support from Cnes. Near real-time altimetry data from the Colorado Center for Astrodynamics Research (CCAR) at the University of Colorado helped in determining the location of the eddy during the research cruises. This publication is partially funded by the Joint Institute for the Study of the Atmosphere and Ocean (JISAO) under NOAA Cooperative Agreement No. NA17RJ1232, Contribution No. 1380. This is contribution no. 513 to the US GLOBEC program, jointly funded by the National Science Foundation and National Oceanic and Atmospheric Administration, contribution FOCI-G584 to Fisheries-Oceanography Coordinated Investigations, and PMEL contribution no. 2898.

### References

- Anderson, L.A., Sarmiento, J.L., 1994. Redfield ratios of remineralization determined by nutrient data analysis. *Global Biogeochemical Cycles* 8, 65–80.
- Aydin, M., Top, Z., Fine, R.A., Olson, D.B., 1998. Modification of the intermediate waters in the northeastern subpolar Pacific. *Journal of Geophysical Research—Oceans* 103, 30923–30940.
- Aydin, M., Top, Z., Olson, D.B., 2004. Exchange processes and watermass modifications along the subarctic front in the North Pacific: oxygen consumption rates and net carbon flux. *Journal of Marine Research* 62, 153–167.
- Batten, S.D., Crawford, W.R., 2005. The influence of coastal origin eddies on oceanic plankton distributions in the eastern Gulf of Alaska. *Deep-Sea Research II* 52, 991–1009.
- Bidle, K.D., Manganelli, M., Azam, F., 2002. Regulation of oceanic silicon and carbon preservation by temperature control on bacteria. *Science* 298, 1980–1984.
- Bograd, S.J., Thomson, R.E., Rabinovich, A.B., LeBlond, P.H., 1999. Near-surface circulation of the northeast Pacific Ocean derived from WOCE-SVP satellite-tracked drifters. *Deep-Sea Research II* 46, 2371–2403.
- Brickley, P.J., Thomas, A.C., 2004. Satellite-measured seasonal and inter-annual chlorophyll variability in the Northeast Pacific and Coastal Gulf of Alaska. *Deep-Sea Research II* 51, 229–245.
- Crawford, W.R., 2005. Heat and fresh water transport by eddies into the Gulf of Alaska. *Deep-Sea Research II* 52, 893–908.
- Crawford, W.R., Cherniawsky, J.Y., Foreman, M.G.G., 2000. Multi-year meanders and eddies in the Alaskan Stream as observed by TOPEX/Poseidon altimeter. *Geophysical Research Letters* 27, 1025–1028.

- Crawford, W.R., Brickley, P.J., Peterson, T.D., Thomas, A.C., 2005. Impact of Haida eddies on chlorophyll distribution in the eastern Gulf of Alaska. *Deep-Sea Research II* 52, 975–989.
- Ducet, N., Le Traon, P.Y., Reverdin, G., 2000. Global high-resolution mapping of ocean circulation from TOPEX/Poseidon and ERS-1 and-2. *Journal of Geophysical Research—Oceans* 105, 19477–19498.
- Favorite, F., Dodimead, A.J., Nasu, K., 1976. Oceanography of the Subarctic Pacific Region, 1960–71. International North Pacific Fisheries Commission, Bulletin 33, 187p.
- Feely, R.A., Sabine, C.L., Schlitzer, R., Bullister, J.L., Mecking, S., Greeley, D., 2004. Oxygen utilization and organic carbon remineralization in the upper water column of the Pacific Ocean. *Journal of Oceanography* 60, 45–52.
- Gordon, L.I., Jennings Jr., J.C., Ross, A.A., Krest, J.M., 1994. A suggested protocol for continuous flow automated analysis of seawater nutrients (phosphate, nitrate, nitrite, and silicic acid) in the WOCE Hydrographic Program and the Joint Global Ocean Fluxes Study. WHP Office Report WHP0 91-1, Part 3.1.3: WHP Operations and Methods, WOCE Report No. 68/91, WOCE Hydrographic Program Office, 52.
- Healey, M.C., Thomson, K.A., Leblond, P.H., Huato, L., Hinch, S.G., Walters, C.J., 2000. Computer simulations of the effects of the Sitka eddy on the migration of sockeye salmon returning to British Columbia. *Fisheries Oceanography* 9, 271–281.
- Joyce, T.M., Patterson, S.L., Millard Jr., R.C., 1981. Anatomy of a cyclonic ring in the Drake Passage. *Deep-Sea Research* 28A, 1265–1287.
- Kalnay, E., Kanamitsu, M., Kistler, R., Collins, W., Deaven, D., Gandin, L., Iredell, M., Saha, S., White, G., Woollen, J., Zhu, Y., Leetmaa, A., Reynolds, B., Chelliah, M., Ebisuzaki, W., Higgins, W., Janowiak, J., Mo, K.C., Ropelewski, C., Wang, J., Jenne, R., Joseph, D., 1996. The NCEP/NCAR 40-Year Reanalysis Project. *Bulletin of the American Meteorological Society* 77, 437–472.
- Kjørboe, T., 2003. High turnover rates of copepod fecal pellets due to *Noctiluca scintillans* grazing. *Marine Ecology Progress Series* 258, 181–188.
- Ladd, C., Stabeno, P., Cokelet, E.D., 2005a. A note on cross-shelf exchange in the northern Gulf of Alaska. *Deep-Sea Research II* 52, 667–679.
- Ladd, C., Kachel, N.B., Mordy, C.W., Stabeno, P.J., 2005b. Observations from a Yakutat eddy in the northern Gulf of Alaska. *Journal of Geophysical Research—Oceans* 110, C03003.
- Le Traon, P.Y., Dibarboure, G., 1999. Mesoscale mapping capabilities of multi-satellite altimeter missions. *Journal of Atmospheric and Oceanic Technology* 16, 1208–1223.
- Le Traon, P.Y., Dibarboure, G., 2004. An illustration of the contribution of the TOPEX/Poseidon-Jason-1 tandem mission to mesoscale variability studies. *Marine Geodesy* 27, 3–13.
- Le Traon, P.Y., Nadal, F., Ducet, N., 1998. An improved mapping method of multi-satellite altimeter data. *Journal of Atmospheric and Oceanic Technology* 15, 522–534.
- Mackas, D.L., Galbraith, M.D., 2002. Zooplankton distribution and dynamics in a North Pacific eddy of coastal origin: I. Transport and loss of continental margin species. *Journal of Oceanography* 58, 725–738.
- Mackas, D.L., Tsurumi, M., Galbraith, M.D., Yelland, D.R., 2005. Zooplankton distribution and dynamics in a North Pacific Eddy of coastal origin: II. Mechanisms of eddy colonization by and retention of offshore species. *Deep-Sea Research II* 52, 1011–1035.
- Musgrave, D.L., Weingartner, T.J., Royer, T.C., 1992. Circulation and hydrography in the northwestern Gulf of Alaska. *Deep-Sea Research* 39, 1499–1519.
- Nelson, D.M., Tréguer, P., Brzezinski, M.A., Leynaert, A., Quéguiner, B., 1995. Production and dissolution of biogenic silica in the ocean: revised global estimates, comparison with regional data and relationship to biogenic sedimentation. *Global Biogeochemical Cycles* 9, 359–372.
- Niiler, P.P., Sybrandt, A.S., Bi, K., Poulain, P.M., Bitterman, D., 1995. Measurements of the water-following capability of holey-sock and TRISTAR drifters. *Deep-Sea Research I* 42, 1951–1955.
- Okkonen, S.R., Jacobs, G.A., Metzger, E.J., Hurlburt, H.E., Shriver, J.F., 2001. Mesoscale variability in the boundary currents of the Alaska Gyre. *Continental Shelf Research* 21, 1219–1236.
- Okkonen, S.R., Weingartner, T.J., Danielson, S.L., Musgrave, D.L., Schmidt, G.M., 2003. Satellite and hydrographic observations of eddy-induced shelf-slope exchange in the northwestern Gulf of Alaska. *Journal of Geophysical Research* 108, 3033.
- Pilskaln, C.H., Lehmann, C., Paduan, J.B., Silver, M.W., 1998. Spatial and temporal dynamics in marine aggregate abundance, sinking rate and flux: Monterey Bay, central California. *Deep-Sea Research II* 45, 1803–1837.
- Ragueneau, O., Tréguer, P., Leynaert, A., Anderson, R.F., Brzezinski, M.A., DeMaster, D.J., Dugdale, R.C., Dymond, J., Fischer, G., François, R., Heinze, C., Maier-Reimer, E., Martin-Jézéquel, V., Nelson, D.M., Quéguiner, B., 2000. A review of the Si cycle in the modern ocean: recent progress and missing gaps in the application of biogenic opal as a. *Global and Planetary Change* 26, 317–365.
- Ream, R.R., Sterling, J.T., Loughlin, T.R., 2005. Oceanographic features related to northern fur seal migratory movements. *Deep-Sea Research II* 52, 823–843.
- Reed, R.K., Stabeno, P.J., 1989. Recent observations of variability in the path and vertical structure of the Alaskan Stream. *Journal of Physical Oceanography* 19, 1634–1642.
- Smetacek, V., 1980. Zooplankton standing stock, copepod faecal pellets and particulate detritus in Kiel Bight. *Estuarine and Coastal Marine Science* 11, 477–490.
- SSALTO/DUACS, 2006. SSALTO/DUACS User Handbook: (M)SLA and (M)ADT Near-Real Time and Delayed Time Products. 47p.
- Tabata, S., 1982. The anticyclonic, baroclinic eddy off Sitka, Alaska, in the northeast Pacific Ocean. *Journal of Physical Oceanography* 12, 1260–1282.
- van Ballegooyen, R.C., Gründlingh, M.L., Lutjeharms, J.R.E., 1994. Eddy fluxes of heat and salt from the southwest Indian Ocean into the southeast Atlantic Ocean: a case study. *Journal of Geophysical Research—Oceans* 99, 14053–14070.
- Van Cappellen, P., Dixit, S., van Beusekom, J., 2002. Biogenic silica dissolution in the oceans: reconciling experimental and field-based dissolution rates. *Global Biogeochemical Cycles* 16, 1075.

- Viitasalo, M., Rosenberg, M., Heiskanen, A.S., Koski, M., 1999. Sedimentation of copepod fecal material in the coastal northern Baltic Sea: where did all the pellets go? *Limnology and Oceanography* 44, 1388–1399.
- Walsh, I.D., Gardner, W.D., 1992. A comparison of aggregate profiles with sediment trap fluxes. *Deep-Sea Research A* 39, 1817–1834.
- Warner, M.J., Bullister, J.L., Wisegarver, D.P., Gammon, R.H., Weiss, R.F., 1996. Basin-wide distributions of chlorofluorocarbons CFC-11 and CFC-12 in the North Pacific: 1985–1989. *Journal of Geophysical Research C: Oceans* 101, 20525–20542.
- Weingartner, T.J., Danielson, S.L., Royer, T.C., 2005. Freshwater variability and predictability in the Alaska Coastal Current. *Deep-Sea Research II* 52, 169–191.